Design and Development of Low Torque Ripple Variable-Speed Drive System with Six-Phase Switched Reluctance Motors

Xu Deng, Barrie Mecrow, *Member, IEEE*, Haimeng Wu, *Member, IEEE* and Richard Martin

***Abstract*—Switched Reluctance Motor (SRM) drives conventionally use current control techniques at low speed and voltage control techniques at high speed. However, these conventional methods usually fail to restrain the torque ripple which is normally associated with this type of machine. Compared with conventional three-phase SRMs, higher phase SRMs have the advantage of lower torque ripple: to further reduce their torque ripple, this paper presents a control method for torque ripple reduction in six-phase SRM drives. A constant instantaneous torque is obtained by regulating the rotational speed of the stator flux linkage. This torque control method is subsequently developed for a conventional converter and a proposed novel converter with fewer switching devices. Moreover, modeling and simulation of this six-phase SRM drive system has been conducted in detail and validated experimentally using a 4.0-kW six-phase SRM drive system. Test results demonstrate that the proposed torque control method has outstanding performance of restraining the torque ripple with both converters for the six-phase SRM, showing superior performance to the conventional control techniques.**

***Index Terms*— Multi-phase, Power converter, Switched reluctance machine, Torque control method, Torque ripple reduction**

I. INTRODUCTION

SWITCHED Reluctance Motors (SRMs) and their drive systems have the advantages of simple structure, low manufacturing cost, high system reliability, high efficiency and a wide speed range, and are contenders for electric vehicle traction drives [1-3]. In recent years they have also been developed for the aviation industry [4-6].

Due to their doubly salient structure SRMs are characterized by strong nonlinearity, resulting in significant torque ripple, which forms the biggest drawback of these machines [7]. Each phase produces a single pulse of torque per electrical cycle, unlike ac machines, which produce two. Thus, with fewer torque pulses per cycle, there tend to be torque dips between pulses. The torque ripple can be 70% and higher in three-phase SRMs [8, 9], and 50% or more in four-phase SRMs [10-12]. Many investigations have sought to reduce the torque ripple: these can be classified into two fields, one based upon machine design optimization and one upon control algorithms.

Design parameters of the machine, for instance the air gap, dimension of the core back, winding arrangement and pole shape have a significant impact upon torque ripple [13]. Many researchers focused on modifying the geometry to minimize torque ripple [14-16]. Increased phase numbers can be used to advantage [17]. By introducing more pulses per cycle they reduce torque ripple, lower the DC link current harmonics and have higher fault-tolerance. However, the added complexity of the high number of power devices and connections to the machine have limited the application.

A six-phase SRM was recently designed and driven by a three-phase full bridge inverter. Compared with a conventional three-phase SRM, it produced lower torque ripple, and with the use of diodes, can still had unidirectional current in each phase [18-20]. More recently a converter topology is proposed by the authors which only consists of six switches, and with which conventional control techniques for SRM drives are applicable[21]. However, this six-phase SRM drive still suffers from obvious torque ripple. Therefore, an effective torque ripple reduction method is desirable for this six-phase SRM drive.

In addition to making geometric changes, the torque ripple can be further decreased by employing an advanced torque ripple reduction control technique. Torque Sharing Functions (TSF) and Direct Instantaneous Torque Control (DITC) have been developed with some success to produce more uniform torque production for three-phase SRMs [22-27]. With the TSF the overall torque demand is distributed to each single phase. By controlling the phase current profile according to the single phase torque demand torque ripple appearing between commutation was reduced [22]. Many different TSFs have been applied to reduce torque ripple for a three-phase SRM [23]: both offline and online TSFs have been investigated, and the torque ripple of the three-phase SRM has been reduced to 40% [25]. A DITC method has also been employed in three-phase SRMs to reduce the torque ripple to 40% and lower [26, 27]. Unlike the TSF method, this latter method does not require a high-precision rotor position sensor. DITC comprises a digital torque hysteresis controller, which generates the switching signals for all activated machine phases. A hysteresis controller regulates the estimated torque of one phase. During phase

Xu Deng, Barrie Mecrow and Haimeng Wu are with Electrical Power Group, School of Engineering, Newcastle University, NE1 7RU, UK. (e-mail: xu.deng@ncl.ac.uk, barrie.mecrow@ncl.ac.uk, haimeng.wu@ncl.ac.uk).
Richard Martin is with Nidec SR Drives Ltd, East Part House, Otley Road, Harrogate, HG3 1PR, UK. (e-mail:richard.martin@nidec-motor.com)

commutation, the torque of two adjacent phases is controlled indirectly by controlling the total torque.

Although both of the above two methods give good reductions in torque ripple in three-phase drives, there are obstacles to their application in six-phase SRMs. For six-phase SRMs, there are always three/four phases conducting simultaneously, so it is much more complex distributing the torque contributions to three or four phases directly. Despite the simple structure of DITC, it requires complex switching rules for smooth torque generation during commutation, which become much more complex again in six-phase SRMs.

The concept of Direct Torque Control (DTC) for ac machines [28, 29] has been developed in SRM drives [30, 31] to simplify the control algorithm and improve the torque response. The nonlinear characteristics and non-sinusoidal excitation of SRMs has hitherto been an obstacle to its application in SRM drives. A DTC methodology was produced for three-phase SRMs from analysis of the nonlinear torque characteristics [30]. This method does not require stator winding modification and can work with unipolar drives. It uses a flux hysteresis controller to keep a constant magnitude of the stator flux, whose vector is accelerated or decelerated to control the instantaneous torque. Simulation showed that under this very simple control algorithm torque ripple in a three-phase SRM is reduced.

The DTC method is well-adapted to multi-phase SRMs because it considers the machine as a whole: by simply increasing the number of voltage vectors, it can be easily developed for higher phase number SRMs. The application of this DTC method to such machines has been simulated [31, 32], but all previous publications on this topic are purely simulation based or at very low speed.

In this paper a torque control method is proposed for six-phase SRM drives with two different converters. The paper is organized as follows. The six-phase SRM prototype, its converters and the torque ripple existing in SRM drive systems are illustrated in Section II. In Section III, the principle of the torque ripple reduction method is introduced and applied to the conventional converter and the proposed converter. Firstly the stator flux definition and the selection rule of voltage vectors are demonstrated with the six-phase conventional converter. Following this, considering the phase independence, the control method for the proposed converter is introduced. Afterwards the performance of the control method is verified with detailed simulation. To further validate the proposed torque control method, a six-phase SRM test rig is constructed for experimental verification in Section IV. Experimental results show a significant reduction in torque ripple throughout the whole speed range when the proposed method is applied. Section V concludes this paper.

II. The Six –phase SRM and Its Converters

It is well understood that increasing the number of phases reduces torque ripple. Thus a six-phase 12/10 SRM is proposed in Fig. 1. Table I gives the design parameters for this machine.

Asymmetric Half Bridge (AHB) converters are the most popular choice for SRM drives because they give independent control of each phase. Fig. 2 shows a six-phase AHB power inverter. Note that this requires twelve controlled switches and twelve diodes – double that of a standard six pulse, three phase ac drive – adding complexity and cost.

(a) (b)

Fig. 1. Six-phase 12/10 SRM prototype. (a) Wound stator. (b) Rotor.

TABLE I.
DESIGN PARAMETERS OF THE SIX-PHASE SRM PROTOTYPE

Number of Rotor Teeth	10	Rated torque	20.0 N·m
Number of Stator Teeth	12	Rated speed	1000 r/min
Phase number	6		

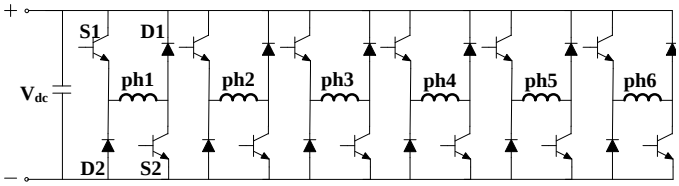

Fig. 2. An asymmetric half bridge converter for six-phase SRMs

The conventional Current Chopping Control (CCC) is first simulated with the AHB converter. The simulation parameters were set as follows: DC link voltage V_{dc} of 200 V; rotation speed n of 200 r/min; current reference I^* of 15.0 A; turn-on θ_{on} and turn-off angle θ_{off} are 0 º and 160º respectively, where 0º corresponds to the unaligned position. Simulated six phase current, flux linkage and torque and the overall instantaneous torque waveforms are shown in Fig. 3. Producing 20.1 N·m average torque, the TRR (Torque Ripple Ratio) under the conventional method is 40.1%.

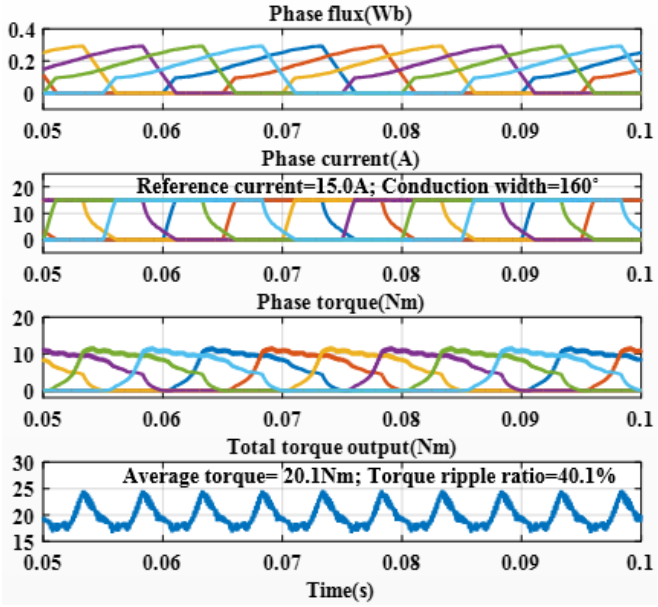

Fig. 3. Simulation waveforms with the AHB converter under the CCC method

Although the cost of a six-phase SRM is no different to that of a three or four-phase SRM, the cost of the drive system is

This article has been accepted for publication in a future issue of this journal, but has not been fully edited. Content may change prior to final publication. Citation information: DOI 10.1109/TEC.2017.2753286, IEEE Transactions on Energy Conversion

higher due to more switching devices and high frequency drive circuits. In order to reduce the quantity of switching devices and connections between the SRM and the inverter the authors proposed a novel converter in [21]. The converter topology is shown in Fig. 4. Conventional control techniques for SRM drives are also applicable to this converter, which has half the number of power devices.

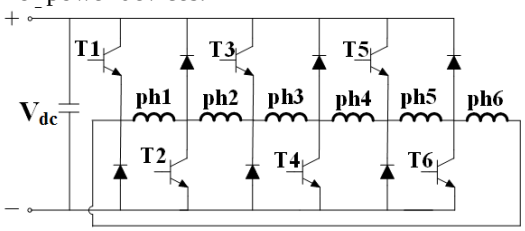

Fig. 4. The proposed converter topology for six-phase SRMs

Simulation under the CCC method with the proposed converter is subsequently conducted. In order to guarantee enough magnetization energy, the switching signals for the six switches in the proposed converter are the logical OR operation results of every adjacent two single phase switching demand. For example, with reference to Fig. 4, if either phase 2, phase 3 or both demand a positive voltage then T3 is switched on. Similarly, if either phase 1 or phase 2 demand a positive voltage then T2 is switched on. Due to the special electrical connection of the proposed converter, there is no longer complete independence of phase voltages: this leads to current distortion when controlled using the CCC method. For an average torque output of 20.0 N·m, the TRR is 32.1% in Fig. 5. Clearly torque ripple of the AHB and the proposed converter is high when using conventional control method and needs to be further reduced.

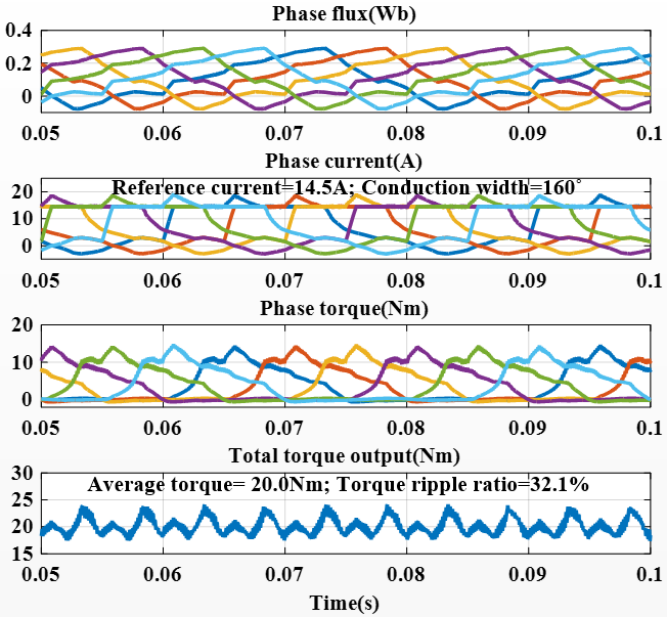

Fig. 5. Simulation waveforms with the proposed converter under the CCC method.

III. Proposed Torque Control Method for Six-phase SRM Drives

Torque in a SRM is generated by excitation current pulses coordinated with the rotor position. The adjustment and timing of excitation currents are regulated by the drive circuit and the torque control techniques. The conventional control methods can vary the mean torque, but because of its highly nonlinear electromagnetic characteristics, even the high phase number SRMs still suffer from torque ripple. As shown in Fig. 3 and Fig. 5, deviations from the mean torque are particularly large near the phase commutation points. To solve this problem an instantaneous torque control method has been investigated.

A. Fundamental principle

To control the instantaneous torque, the nonlinear torque characteristics have to be derived. Fig. 6 shows the determination of electromagnetic torque considering saturation.

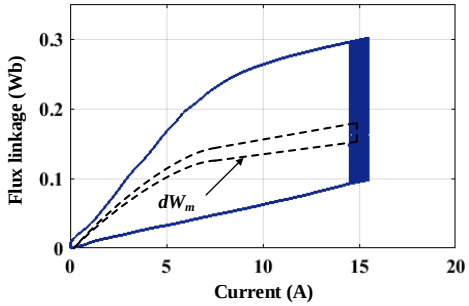

Fig. 6. Determination of electromagnetic torque

The average output torque is determined by

$$T_{av} = \frac{dW_m}{d\theta} \tag{1}$$

Here the current is assumed to be constant during a small displacement $d\theta$, because a first order delay exists in phase current variation with respect to the phase voltage and the stator flux linkage variation [30]. Ignoring the resistive loss, the energy exchanged with the supply dW_e is given in (2), and the change of mechanical energy dW_m is what is left after the change of magnetic stored energy dW_f as (3).

$$\begin{aligned} dW_e &= \int (V - iR) i dt \\ &= \int \left(\frac{\partial \psi}{\partial i}\frac{di}{dt} + \frac{\partial \psi}{\partial \theta}\frac{d\theta}{dt}\right) i dt \\ &= \int i \frac{\partial \psi}{\partial \theta} \omega_m dt \end{aligned} \tag{2}$$

$$dW_m = dW_e - dW_f \tag{3}$$

Therefore, the change of mechanical energy is the area surrounded by the dashed line in Fig. 6 which equals to $T_e d\theta$, so that instantaneous output torque can be expressed as (4)

$$\begin{aligned} T_e &= \left.\frac{dW_m}{d\theta}\right|_{i=const} = \left.\frac{d(W_e - W_f)}{d\theta}\right|_{i=const} \\ &= \left.\frac{dW_e}{d\theta}\right|_{i=const} - \left.\frac{dW_f}{d\theta}\right|_{i=const} \\ &= i\left.\frac{\partial \psi(\theta, i)}{\partial \theta}\right|_{i=const} - \left.\frac{\partial W_f}{\partial \theta}\right|_{i=const} \end{aligned} \tag{4}$$

Since the changing ratio of the magnetic stored energy is always less than the first term in (4), it can be further simplified as:

$$T_e \approx i\left.\frac{\partial \psi(\theta, i)}{\partial \theta}\right|_{i=const} \tag{5}$$

This article has been accepted for publication in a future issue of this journal, but has not been fully edited. Content may change prior to final publication. Citation information: DOI 10.1109/TEC.2017.2753286, IEEE Transactions on Energy Conversion

As current is assumed to be a constant, the second term of (5) is expressed as:

$$A = \left.\frac{\partial \psi(\theta, i)}{\partial \theta}\right|_{i=const} \tag{6}$$

Where the change of instantaneous torque T_e is completely dependent on the value of (6). To simplify the analysis with (5), assuming stator flux ψ can be controlled as constant, then the change of T_e only depends on the velocity change of ψ with respect to rotor position. Therefore an increasing value of (6) is defined as flux acceleration, whereas a decreasing value of (6) is defined as flux deceleration. Hence, this control method for SRMs contains two essential factors: 1) choose a proper method to keep the magnitude of the stator flux linkage constant; 2) accelerate or decelerate the rotational stator flux to control the overall torque.

B. Developed torque control method for the six-phase AHB converter

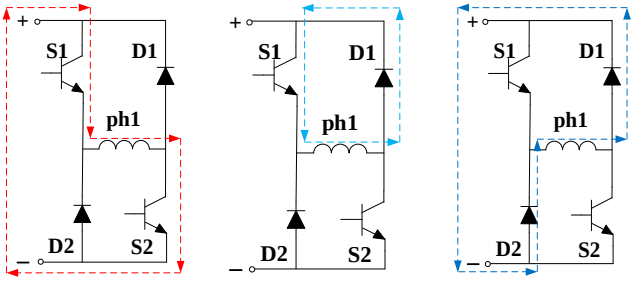

Fig. 7. Phase voltage states in the AHB converter.

Depending on the on-off states of switches, there are three voltage states for each phase in the AHB converter as shown in Fig. 7. Afterward, voltage vectors are employed to represent a combination of all the six phase switching states at different instant. However, switching states in SRMs are time functions and they have no relevant relationship with the stator flux space vector.

In order to build a relationship between switching states and the stator flux space vector for further investigation, the voltage vector direction of each phase is selected along the direction of the phase flux vector in the time-space coordinate system. However, for each phase there are three voltage states, thus for six phase SRMs there are huge quantity of voltage vectors, which increases the complexity of this method. Therefore, the first task is to find some reasonable voltage vectors. Based on the original electrical design of the six-phase SRMs, there are three or two adjacent phases working simultaneously. Thus reasonable voltage vectors can be selected as follows.

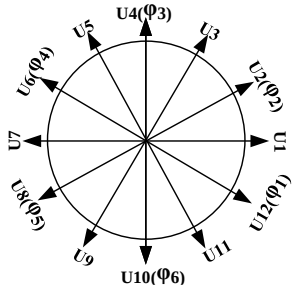

U1 (+1,+1,-1,-1,-1,-1)
U2 (+1,+1,+1,-1,-1,-1)
U3 (-1,+1,+1,-1,-1,-1)
U4 (-1,+1,+1,+1,-1,-1)
U5 (-1,-1,+1,+1,-1,-1)
U6 (-1,-1,+1,+1,+1,-1)
U7 (-1,-1,-1,+1,+1,-1)
U8 (-1,-1,-1,+1,+1,+1)
U9 (-1,-1,-1,-1,+1,+1)
U10 (+1,-1,-1,-1,+1,+1)
U11 (+1,-1,-1,-1,-1,+1)
U12 (+1,+1,-1,-1,-1,+1)

Fig. 8. Determination of voltage vectors

As shown in Fig. 8, U2, U4, U6, U8, U10, and U12 have the same voltage directions as phases 1 to 6, and there are three adjacent phases conducting simultaneously. For more flexible control, the six-phase SRM employs six extra voltage vectors. To achieve a balanced voltage vector arrangement, the extra six voltage vectors U1, U3, U5, U7, U9, and U11 are designed.

According to the stator flux relationship shown in Fig. 9, the amplitude of the stator flux is a combination value of the six phase fluxes according to (7), (8) and (9). The position of the stator flux is calculated by (10).

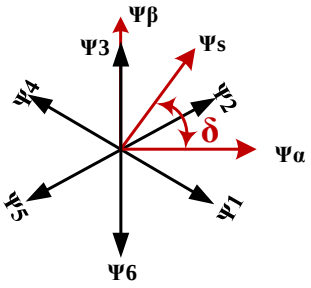

Fig. 9. Determination of stator flux

$$\psi_\alpha = (\psi_1 + \psi_2 - \psi_4 - \psi_5)\cos 30° \tag{7}$$

$$\psi_\beta = (-\psi_1 + \psi_2 + \psi_4 - \psi_5)\sin 30° + \psi_3 - \psi_6 \tag{8}$$

$$\psi_s = \sqrt{\psi_\alpha^2 + \psi_\beta^2} \tag{9}$$

$$\delta = \arctan\left(\frac{\psi_\beta}{\psi_\alpha}\right) \tag{10}$$

To locate the stator flux the vector space is segmented into twelve zones. As shown in Fig. 10, each zone occupies 30º and the voltage vectors are respectively positioned in the central axis of the corresponding zones.

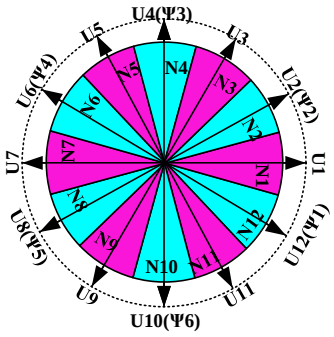

N1=[-15º, +15º]
N2=[+15º, +45º]
N3=[+45º, +75º]
N4=[+75º, +105º]
N5=[+105º, +135º]
N6=[+135º,+165º]
N7=[+165º, +180º]∪[-180º, -165º]
N8=[-165º, -135º]
N9=[-135º, -105º]
N10=[-105º, -75º]
N11=[-75º, -45º]
N12=[-45º, -15º]

Fig. 10. Zones arrangement

On the basis of the proposed control method, the amplitude and rotational speed of the flux vector is regulated by means of choosing a proper voltage vector. Owing to this, the stator flux expression is shown in differential form:

$$\Psi(k) = \Psi(k-1) + U(k)T_s \tag{11}$$

Where T_s is the sample time.

The relationship between the stator flux and voltage vectors is shown in Fig. 11. If the angle between these two vectors is acute, the voltage vector U(k) has a component along the positive direction of Ψ(k-1) and the flux magnitude increases, whereas if the angle is obtuse, U(k) has component along the negative direction of Ψ(k-1) and the flux amplitude decreases.

This article has been accepted for publication in a future issue of this journal, but has not been fully edited. Content may change prior to final publication. Citation information: DOI 10.1109/TEC.2017.2753286, IEEE Transactions on Energy Conversion

In addition, when the voltage vector U(k) is at an angle in advance of the stator flux vector, the stator flux is advanced. Providing the advance is also positive with respect to rotor electrical position, the instantaneous torque T_e increases according to (5), and vice versa.

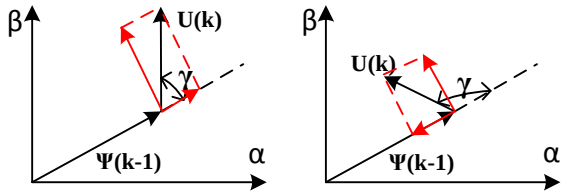

Fig. 11. Relationship between stator flux and voltage vectors

According to the above analysis, amplitudes of stator flux and instantaneous torque are regulated by switching proper voltage vectors. For example, if the stator flux is in zone N1 and is smaller than the command value, voltage vectors U2, U3, U11 and U12, which have an acute angle with the stator flux, are selected. If stator flux is larger than command value, voltage vectors U5, U6, U7, U8 and U9, which have obtuse angle with the stator flux, are selected. The adjustment of the instantaneous torque can also be determined according to whether the voltage vector leads or lags the stator flux vector.

To implement this control concept, the torque demand and the stator flux demand have to be considered simultaneously. Generally, if torque and flux are to rise the voltage vector can be selected in one zone ahead. To increase stator flux whilst instantaneous torque is to fall, the voltage vector can be chosen in two zones behind. To increase torque and decrease flux, the voltage should be chosen in four zones ahead. If torque and flux are to fall the voltage vector should be selected in five zones behind. Consequently the switching rule for the six-phase SRM with the AHB converter is summarized in Table II, where k is zone number where the stator flux locates.

TABLE II.
SWITCHING RULE OF THE SIX-PHASE AHB CONVERTER

Ψ↑T↑	Ψ↓T↓	Ψ↑T↓	Ψ↓T↑
U(k+1)	U(k-5)	U(k-2)	U(k+4)

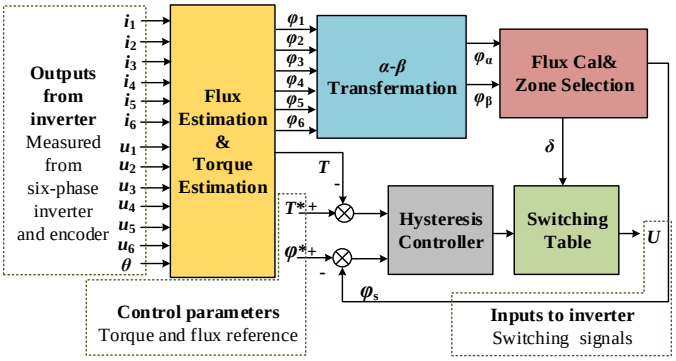

Fig. 12. Control diagram of the proposed torque control method for six-phase SRMs

Fig. 12 shows the control diagram of the proposed torque control method for six-phase SRMs, in which control parameters are instantaneous torque and stator flux linkage. Six phase flux amplitudes are obtained from integration of the phase voltage according to (11), and therefore the amplitude and angular position of the stator flux vector is calculated according to (7), (8), (9) and (10) in the flux estimation block. Estimated torque is calculated using measured nonlinear magnetization characteristics of the prototype when phase current and rotor position are available from a current sensor and position encoder. Two hysteresis controllers are employed in this control system for torque and stator flux linkage amplitude regulation. The regulation commands of these two hysteresis controllers are the basis of selecting a proper voltage vector from the switching table during each control cycle.

Fig. 13 shows simulation results under the proposed control method with the AHB converter. The simulation parameters are set as follows: DC link voltage V_{dc} is 200 V; rotation speed n is 200 r/min; the flux linkage reference ψ^* is 0.38 Wb and the torque reference T^* is 20 N·m.

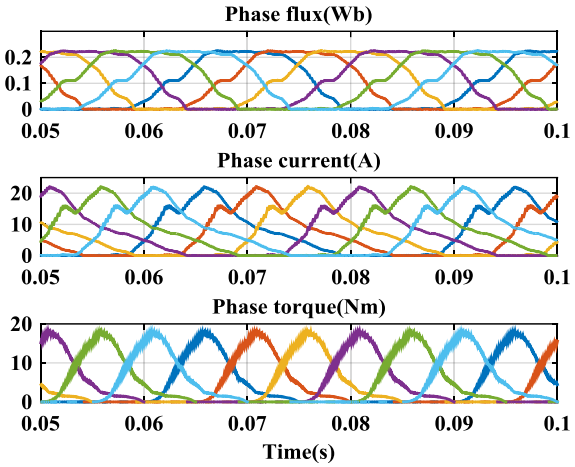

Fig. 13. Simulation waveforms with the AHB converter under the proposed torque control method.

Under the conventional current control method, six phase currents are regulated as approximately square waveforms by current hysteresis controllers. Under the proposed torque control method, switching signals are generated with instantaneous torque and stator flux errors. Compared with the conventional CCC method the phase flux linkage and current are very irregular due to adjustment requirement of the flux and torque hysteresis controllers. Another significant distinction is that both the phase torque and current have larger maximum values under the proposed method, but phase flux is substantially reduced.

Fig. 14 shows the relationship between the change of instantaneous torque and rotational speed. When the flux advances ahead of the rotor movement the torque increases, and when the flux lags behind the rotor movement the torque decreases.

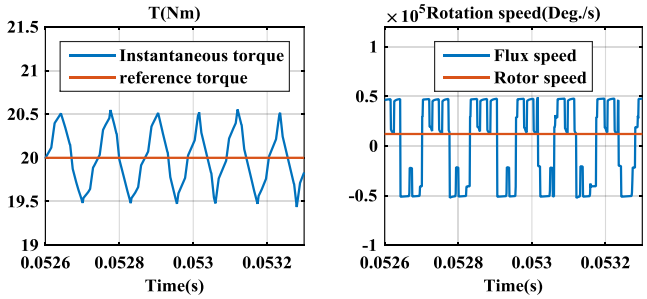

Fig. 14. Instantaneous torque and flux speed of the proposed control method

This article has been accepted for publication in a future issue of this journal, but has not been fully edited. Content may change prior to final publication. Citation information: DOI 10.1109/TEC.2017.2753286, IEEE Transactions on Energy Conversion

For an average torque output of 20.0 N·m, compared with the conventional current control method, the proposed torque control method reduces the TRR from 40.1% to 5.1% as shown in Fig. 15(a). By plotting stator flux vectors of the CCC method and the proposed method in Fig. 15 (b), it is further demonstrated that the stator flux linkage in the CCC method is close to a hexagon, whilst the proposed method has a circular trajectory.

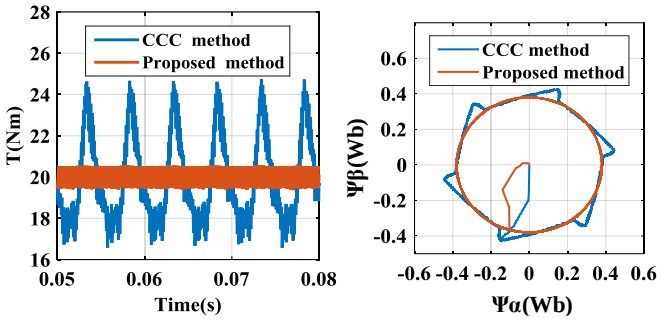

(a) (b)

Fig. 15. Output comparison between the CCC and the proposed method with the AHB converter (a) Total torque output. (b) Flux trajectory.

C. Developed torque control method for the proposed novel converter

In order to reduce the switch number for the six-phase SRM drive, the novel converter has been proposed. As discussed in [21], all conventional control techniques for SRM drives can be used with the proposed novel converter, but torque ripple is as significant as with the AHB converter.

The main distinction between the six-phase AHB converter and the proposed converter is phase independence, therefore the voltage vectors and switching table of the proposed method for the AHB converter cannot be directly applied to the novel converter. For example, U1 in Fig. 8 is (+1,+1,0,-1,-1,0), in which two adjacent phases are conducting and two phases are freewheeling. For the proposed converter, to achieve the same effect, the equivalent voltage vector V1 can be defined as (+1,+1,+1,-1,-1,-1), where '+1' represents the on-state and '-1' represents the off-state for each switch. U2 in Fig. 8 is (+1,+1,+1,-1,-1,-1), in which three adjacent phases are conducting and other phases are non-conducting. For the proposed converter, every switch is shared by two phases. It is obvious that there are always two phases in freewheeling loops, therefore it is impossible to define an equivalent voltage vector with U2. Consequently, there are six reasonable voltage vectors that can be employed with the proposed converter. Table III demonstrates the six voltage vectors for the proposed converter.

TABLE III.

VOLTAGE VECTORS FOR THE PROPOSED CONVERTER

V1(+1,+1,+1,-1,-1,-1)	V3(-1,-1,+1,+1,+1,-1)	V5(+1,-1,-1,-1,+1,+1)
V2(-1,+1,+1,+1,-1,-1)	V4(-1,-1,-1,+1,+1,+1)	V6(+1,+1,-1,-1,-1,+1)

As the quantity of voltage vectors are reduced from twelve to six, the zone arrangement is changed accordingly. In order to locate the stator flux, the vector space is segmented into six zones as shown in Fig. 16, every zone occupies 60º. The stator flux definition is similar to the AHB converter. The amplitude and position of the stator flux vector are calculated by (7) to (10). Stator flux vector and voltage vectors also fulfil the relationships in Fig. 11.

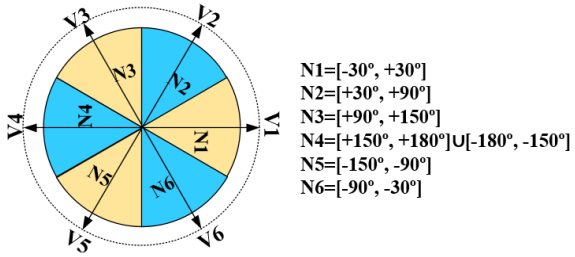

Fig. 16. Zones arrangement for the proposed converter.

Considering demands of the stator flux and torque simultaneously, Table IV shows the switching rule for the proposed converter. If torque and flux are to rise the voltage vector can be selected in one zone ahead. To increase stator flux whilst instantaneous torque is to fall, the voltage vector can be chosen in one zone behind. To increase torque and decrease flux, the voltage should be chosen in two zones ahead. If torque and flux are to fall the voltage vector should be selected in two zones behind.

TABLE IV.

SWITCHING RULE FOR THE PROPOSED CONVERTER

Ψ↑T↑	Ψ↓T↓	Ψ↑T↓	Ψ↓T↑
V(k+1)	V(k-2)	V(k-1)	V(k+2)

Fig. 17 shows simulation results under the proposed method with the novel converter. The simulation parameters are set as follows: DC link voltage V_{dc} is 200 V; rotation speed n is 200r/min; the flux linkage reference ψ^* is 0.38 Wb and the torque reference T^* is 20 N·m.

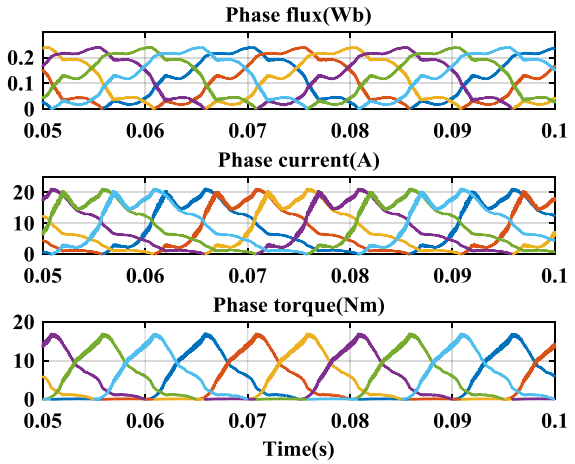

Fig. 17. Simulation waveforms with the proposed converter under the proposed torque control method

Compared with results with the conventional CCC method in Fig. 4, the phase flux linkage and current are very irregular due to an adjustment requirement of the torque and flux hysteresis controllers. Compared with the six-phase AHB converter, different voltage vectors are employed with the proposed converter, thus the current waveforms are slightly different to the AHB converter. However, this does not affect the torque ripple reduction performance of the proposed torque control method.

For an average torque output of 20.0 Nm, compared with the conventional current control method, the proposed torque control method reduces the TRR from 32.1% to 6.8% as shown in Fig. 18(a). By plotting stator flux vectors of two torque control methods in the x-y stationary frame in Fig. 18(b) it is further demonstrated that, as with the AHB converter, the stator flux linkage with the CCC method is close to a hexagon, whilst the proposed torque control method has a circular trajectory.

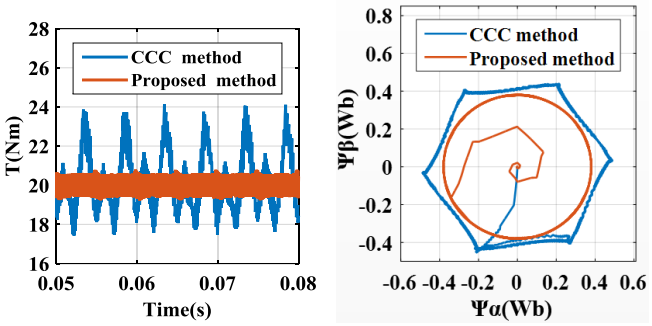

(a) (b)

Fig. 18. Output comparison between the CCC and the proposed method with the proposed converter (a) Total torque output. (b) Flux trajectory.

Comparing the flux trajectory under the proposed torque control method with the AHB converter, the flux trajectory under direct torque control applied to the novel converter has a longer path before it reach the reference value, suggesting that the dynamic torque response may be slower. This is because the voltage vectors employed with the proposed converter only allow two phases conducting simultaneously, whilst the AHB converter allows three, which helps the AHB converter build stator flux linkage faster.

IV. Experimental Validation

In order to implement a real-time low torque ripple six-phase SRM drive system, a six-phase SRM drive system test rig was designed and constructed as shown in Fig. 19. This drive system is made up of a six-phase SRM coupled to a permanent magnet load machine, IGBT inverters, a F28335 digital signal processor (DSP) based controller, a shaft absolute encoder interfaced to the DSP controller, etc.. The winding connection for this machine is so as to ensure there is minimal coupling between phases, caused solely by low levels of cross-slot leakage flux. It was found that the mutual effects could therefore be ignored in this case.

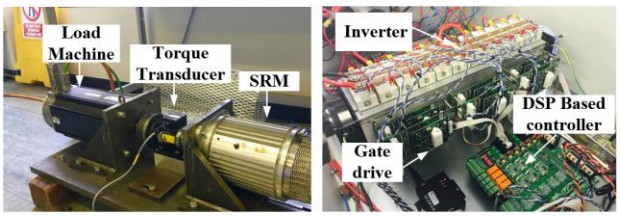

Fig. 19. Test rig set up.

A. Experimental results of the AHB converter

Fig. 20 shows experimental waveforms including phase current and torque output with the AHB converter at 200 r/min, with a mean torque of 20 N·m. Compared with the conventional method, the proposed torque control method reduces the TRR from 29.7% to 12.1%.

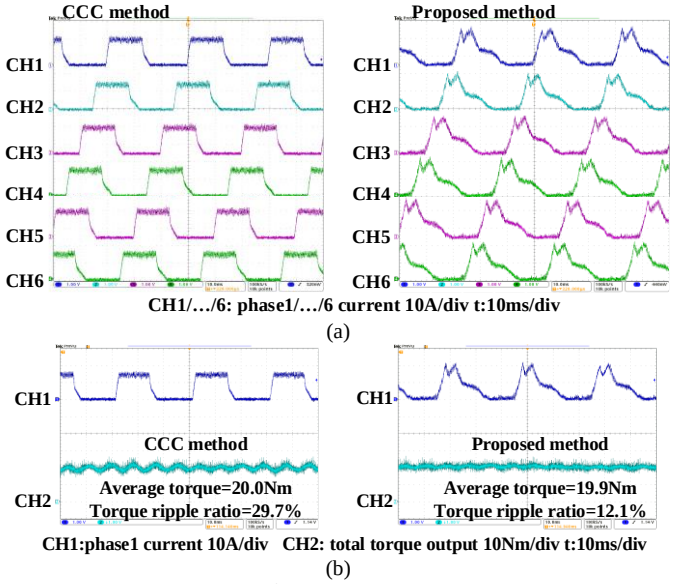

Fig. 20. Experimental waveforms with the AHB converter at 200 r/min (T_{ref}=20 N·m). (a) Six phase current. (b) Torque output.

Fig. 21 shows experimental waveforms including phase current and torque output at 800 r/min and 1500 r/min. With a mean torque of 10 N·m and 15 N·m, the torque ripple with the AHB converter is significantly reduced under the proposed method.

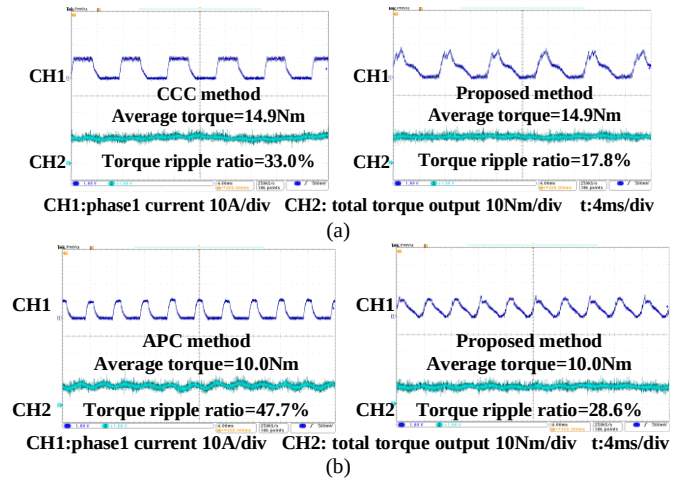

Fig. 21. Experimental waveforms of phase current and torque output of the proposed and conventional control methods with the AHB converter. (a) At 800 r/min (T_{ref}=15 N·m). (b) At 1500 r/min (T_{ref}=10 N·m)

With a mean torque of 14.9 N·m at 800 r/min, the proposed torque control method restrains the TRR to 17.8%, nearly half of the TRR under conventional method. With a mean torque of 10.0 N·m at 1500 r/min, the TRR under the Angle Position Control (APC) method is 47.7%, meanwhile the proposed torque control method restrains the TRR to 28.6%.

B. Experimental results of the proposed converter

Fig. 22 shows experimental waveforms including phase current and torque output with the proposed converter at 200 r/min, with a mean torque of 20 N·m. Compared with the conventional method, the proposed torque control method reduces the TRR from 42.1% to 14.3%.

This article has been accepted for publication in a future issue of this journal, but has not been fully edited. Content may change prior to final publication. Citation information: DOI 10.1109/TEC.2017.2753286, IEEE Transactions on Energy Conversion

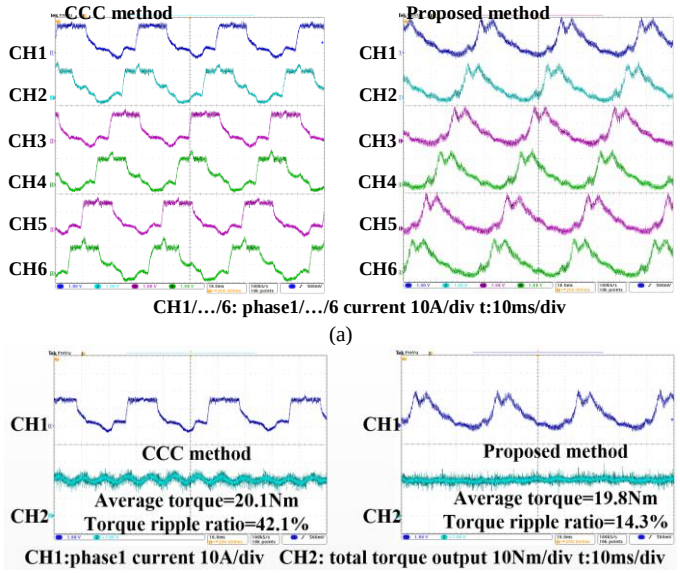

Fig. 22. Experimental waveforms with the proposed converter at 200 r/min (T_{ref}=20 N·m). (a) Six phase current. (b) Torque output.

Fig. 23 shows experimental waveforms including phase current and torque output at 800 r/min and 1500 r/min. With a mean torque of 10 N·m and 15 N·m, the torque ripple with the proposed converter are significantly reduced under the proposed method. With a mean torque of 15.0 N·m at 800 r/min, the proposed torque control method restrains the TRR to 18.5%, lower than half of the TRR under conventional method. With a mean torque of 10.0 N·m at 1500 r/min, the TRR under the Angle Position Control (APC) method is 36.9%, meanwhile the proposed torque control method restrains the TRR to 27.4%.

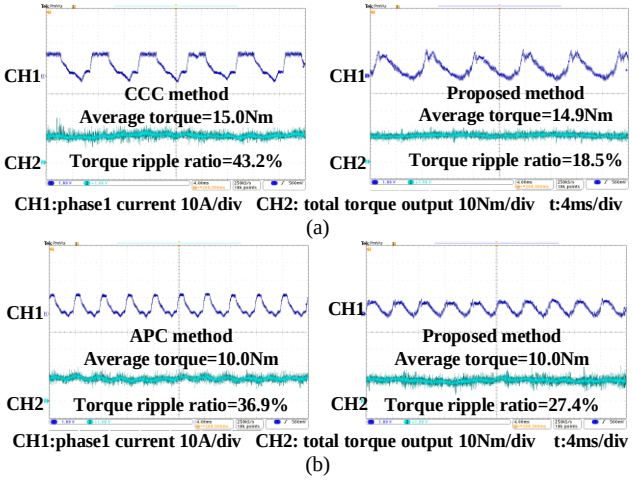

Fig. 23. Experimental waveforms of phase current and torque output of the proposed and conventional control methods with the proposed converter. (a) At 800r/min (T_{ref}=15 N·m). (b) At 1500r/min (T_{ref}=10 N·m)

Consequently, compared with conventional control methods, the proposed torque control method can reduce the torque ripple for six-phase SRMs with both the AHB converter and the proposed converter throughout the whole speed range.

It is noticeable that, whilst the torque ripple predicted by simulation is typically 5% of the mean output torque, the measured torque ripple is generally higher. Simulations revealed that this is caused by cross-saturation effects in the core backs, which are not accounted for in the single phase characteristics used in the controller. Note also that, due to voltage limitations, the demanded rate of change of flux angle will sometimes exceed that which the converter can supply: consequently the torque ripple reduction at high speed is inferior to that at low speed.

In order to compare the torque-speed performance of the proposed low torque ripple drive systems, a 200V, 48A DC power supply is employed. The torque-speed curves are shown in Fig. 24. At low speed the torque is limited by the maximum current from the power supply, whilst at high speed it is limited by the available voltage. The proposed method can produce larger mean torque at low and medium speed because the currents are shaped to give increased torque per amp, whilst the conventional control method can produce larger average torque at high speed because it simply applies full voltage throughout the conduction period.

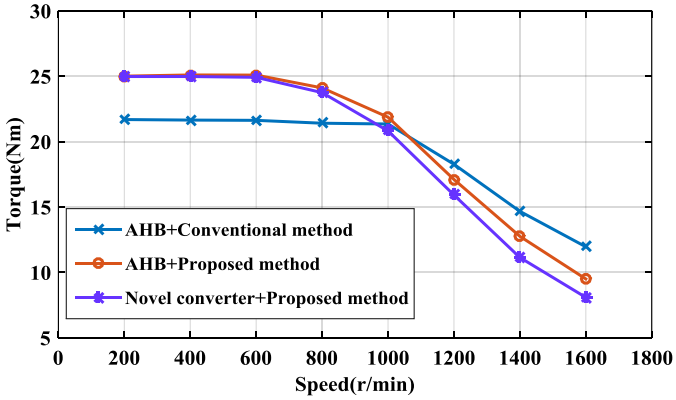

Fig. 24. Torque-Speed performance comparison

V. Conclusion

In this paper, a torque control method for torque ripple reduction has been proposed to control six-phase SRM drive systems. Although six-phase SRMs have lower torque ripple compared with other conventional SRMs, they still suffer from obvious torque ripple. Therefore a torque control method for torque ripple reduction is proposed to further reduce the amount of torque ripple with both conventional and proposed converter.

The proposed torque control method for six-phase SRMs is firstly researched with the six-phase AHB converter. Simulation results verify that the proposed control method with the AHB converter can observably reduce the TRR from 40.1% to 5.1%. Afterwards the proposed method with the proposed converter is investigated. There is reduced phase independence in the proposed converter, consequently a modified torque control method with six voltage vectors is proposed based on the control method designed for the six-phase AHB converter. Although fewer voltage vectors are used with the proposed converter, the torque ripple reduction performance has not been affected. Simulation results verified that the modified control method with the novel converter can reduce the TRR from 32.1% to 6.8%.

Experimental tests have been carried out to validate the torque ripple reduction performance of the proposed control

method. Test results show that the proposed torque control method can reduce torque ripple significantly throughout the whole speed range with both conventional and proposed novel converter.

REFERENCES

[1] R. Madhavan and B. G. Fernandes, "Axial Flux Segmented SRM With a Higher Number of Rotor Segments for Electric Vehicles," *IEEE Transactions on Energy Conversion*, vol. 28, pp. 203-213, 2013.

[2] A. Chiba, K. Kiyota, N. Hoshi, M. Takemoto, and S. Ogasawara, "Development of a Rare-Earth-Free SR Motor With High Torque Density for Hybrid Vehicles," *IEEE Transactions on Energy Conversion*, vol. 30, pp. 175-182, 2015.

[3] B. Fahimi, A. Emadi, and R. B. Sepe, "A switched reluctance machine-based starter/alternator for more electric cars," *IEEE Transactions on Energy Conversion*, vol. 19, pp. 116-124, 2004.

[4] J. Kim, K. Ha, and R. Krishnan, "Single-Controllable-Switch-Based Switched Reluctance Motor Drive for Low Cost, Variable-Speed Applications," *IEEE Transactions on Power Electronics*, vol. 27, pp. 379-387, 2012.

[5] M. Krishnamurthy, C. S. Edrington, A. Emadi, P. Asadi, M. Ehsani, and B. Fahimi, "Making the case for applications of switched reluctance motor technology in automotive products," *IEEE Transactions on Power Electronics*, vol. 21, pp. 659-675, 2006.

[6] Y. Sozer, I. Husain, and D. A. Torrey, "Guidance in Selecting Advanced Control Techniques for Switched Reluctance Machine Drives in Emerging Applications," *IEEE Transactions on Industry Applications*, vol. 51, pp. 4505-4514, 2015.

[7] I. Husain, "Minimization of torque ripple in SRM drives," *IEEE Transactions on Industrial Electronics*, vol. 49, pp. 28-39, 2002.

[8] S. Song, Z. Xia, Z. Zhang, and W. Liu, "Control Performance Analysis and Improvement of a Modular Power Converter for Three-Phase SRM With Y-Connected Windings and Neutral Line," *IEEE Transactions on Industrial Electronics*, vol. 63, pp. 6020-6030, 2016.

[9] A. Klein-Hessling, A. Hofmann, and R. W. D. Doncker, "Direct instantaneous torque and force control: a control approach for switched reluctance machines," *IET Electric Power Applications*, vol. 11, pp. 935-943, 2017.

[10] M. Ćosović, S. Smaka, I. Salihbegović, and M. Š, "Design optimization of 8/14 switched reluctance machine for electric vehicle," in *XXth International Conference on Electrical Machines*, 2012, pp. 2654-2659.

[11] J. Lin, T. Lambert, Y. Yang, B. Bilgin, R. Lankin, and A. Emadi, "A novel axial flux switched reluctance motor with multi-level air gap geometry," in *IEEE Electrical Power and Energy Conference (EPEC)*, 2016, pp. 1-8.

[12] Q. Sun, J. Wu, C. Gan, Y. Hu, N. Jin, and J. Guo, "A New Phase Current Reconstruction Scheme for Four-Phase SRM Drives Using Improved Converter Topology Without Voltage Penalty," *IEEE Transactions on Industrial Electronics*, vol. 45, pp. 1-10, 2017.

[13] R. Krishnan, *Switched Reluctance Motor Drives: Modeling, Simulation, Analysis, Design, and Applications*: Hoboken, 2001.

[14] C. Yong Kwon, Y. Hee Sung, and K. Chang Seop, "Pole-Shape Optimization of a Switched-Reluctance Motor for Torque Ripple Reduction," *IEEE Transactions on Magnetics*, vol. 43, pp. 1797-1800, 2007.

[15] N. K. Sheth and K. R. Rajagopal, "Optimum pole arcs for a switched reluctance motor for higher torque with reduced ripple," *IEEE Transactions on Magnetics*, vol. 39, pp. 3214-3216, 2003.

[16] H. Eskandari and M. Mirsalim, "An Improved 9/12 Two-Phase E-Core Switched Reluctance Machine," *IEEE Transactions on Energy Conversion*, vol. 28, pp. 951-958, 2013.

[17] J. A. Haylock, B. C. Mecrow, A. G. Jack, and D. J. Atkinson, "Operation of a fault tolerant PM drive for an aerospace fuel pump application," *IEE Proceedings on Electric Power Applications*, vol. 145, pp. 441-448, 1998.

[18] J. D. Widmer, B. C. Mecrow, C. M. Spargo, R. Martin, and T. Celik, "Use of a 3 phase full bridge converter to drive a 6 phase switched reluctance machine," in *6th IET International Conference on Power Electronics, Machines and Drives*, 2012, pp. 1-6.

[19] J. D. Widmer, R. Martin, C. M. Spargo, B. C. Mecrow, and T. Celik, "Winding configurations for a six phase switched reluctance machine," in *XXth International Conference on Electrical Machines (ICEM)* 2012, pp. 532-538.

[20] R. Martin, J. D. Widmer, B. C. Mecrow, M. Kimiabeigi, A. Mebarki, and N. L. Brown, "Electromagnetic Considerations for a Six-Phase Switched Reluctance Motor Driven by a Three-Phase Inverter," *IEEE Transactions on Industry Applications*, vol. 52, pp. 3783-3791, 2016.

[21] X. Deng, B. Mecrow, and S. Gadoue, "A novel converter topology for 6 phase switched reluctance motor drives," in *Annual Conference of Industrial Electronics Society*, 2013, pp. 268-273.

[22] V. P. Vujicic, "Minimization of Torque Ripple and Copper Losses in Switched Reluctance Drive," *IEEE Transactions on Power Electronics*, vol. 27, pp. 388-399, 2012.

[23] X. D. Xue, K. W. E. Cheng, and S. L. Ho, "Optimization and Evaluation of Torque-Sharing Functions for Torque Ripple Minimization in Switched Reluctance Motor Drives," *IEEE Transactions on Power Electronics*, vol. 24, pp. 2076-2090, 2009.

[24] Y. Jin, B. Bilgin, and A. Emadi, "An Extended-Speed Low-Ripple Torque Control of Switched Reluctance Motor Drives," *IEEE Transactions on Power Electronics*, vol. 30, pp. 1457-1470, 2015.

[25] Y. Jin, B. Bilgin, and A. Emadi, "An Offline Torque Sharing Function for Torque Ripple Reduction in Switched Reluctance Motor Drives," *IEEE Transactions on Energy Conversion*, vol. 30, pp. 726-735, 2015.

[26] N. H. Fuengwarodsakul, M. Menne, R. B. Inderka, and R. W. D. Doncker, "High-dynamic four-quadrant switched reluctance drive based on DITC," *IEEE Transactions on Industry Applications*, vol. 41, pp. 1232-1242, 2005.

[27] R. B. Inderka and R. W. A. A. D. Doncker, "DITC-direct instantaneous torque control of switched reluctance drives," *IEEE Transactions on Industry Applications*, vol. 39, pp. 1046-1051, 2003.

[28] I. Takahashi and T. Noguchi, "A New Quick-Response and High-Efficiency Control Strategy of an Induction Motor," *IEEE Transactions on Industry Applications*, vol. IA-22, pp. 820-827, 1986.

[29] L. Zhong, M. F. Rahman, W. Y. Hu, and K. W. Lim, "Analysis of direct torque control in permanent magnet synchronous motor drives," *IEEE Transactions on Power Electronics*, vol. 12, pp. 528-536, 1997.

[30] A. D. Cheok and Y. Fukuda, "A new torque and flux control method for switched reluctance motor drives," *IEEE Transactions on Power Electronics*, vol. 17, pp. 543-557, 2002.

[31] P. Chancharoensook, "Direct instantaneous torque control of a four-phase switched reluctance motor," in *International Conference on Power Electronics and Drive Systems*, 2009, pp. 770-777.

[32] R. S. Kumar and J. A. Vasanth, "Intelligent neuro controller based speed and torque control of five phase switched reluctance motor," in *International Conference on Information Communication and Embedded Systems*, 2013, pp. 966-973.

Xu Deng received the B.Eng. and M.Eng. degrees in Electrical Engineering from Nanjing University of Aeronautics and Astronautics, Nanjing, China, in 2010 and 2013, respectively. She received the PhD degree in Electrical Engineering from Newcastle University, Newcastle upon Tyne, U.K, in 2017. She is currently a Research Associate of Electrical Power Research Group in the School of Engineering, Newcastle University, Newcastle upon Tyne, U.K. Her main researches are integrated drives and advanced control methods for power electronics and electric machines.

Barrie Mecrow received the Ph.D. degree in Electrical Engineering from Newcastle University, Newcastle, U.K., in 1986. He was a Turbo-generator Design Engineer at NEI Parsons, Newcastle upon Tyne, U.K. In 1987, he became a Lecturer and in 1998 a Professor at Newcastle University. His research interests include fault-tolerant drives, high-performance permanent

magnet machines, and novel switched reluctance drives.

Haimeng Wu (M'10) was born in Zhejiang, China, in 1986. He received the B.Sc. degree in Electrical Engineering from Chongqing University, Chongqing, China, in 2008. He was nominated as the postgraduate exempted from the national postgraduate entrance examination to Zhejiang University and then he received the M.Sc. degree in Power Electronics from the College of Electrical Engineering, Zhejiang University, Hangzhou, China, in 2011. He received the grants from Engineering and Physical Science Council (EPSRC) for his further education in UK and he had his Ph.D. degree in Power Electronics at the School of Electrical and Electronic Engineering, Newcastle University, United Kingdom in 2016. He has been with the Electrical Power Research Group at Newcastle University as a Postdoctoral Researcher since 2015. His current research interests include power electronics for electric vehicles, design and advanced nonlinear control of power converters, health monitoring techniques.

Richard Martin received the M.Eng. degree in general engineering and the Ph.D. degree in Electrical Engineering from the University of Durham, Durham, U.K., in 2002 and 2007, respectively. He was a Research Associate with Newcastle University, Newcastle, U.K. from 2012 to 2016 and is now an Electromagnetic Design Engineer with Nidec SR Drives Ltd., Harrogate, U.K.